DØ Note 5722-CONF

Model-independent measurement of the W boson helicity in top quark decays at D0

The DØ Collaboration

(Dated: July 25, 2008)

We present a model-independent measurement of the helicity of W bosons produced in top quark decays, based on a data sample of up to 2.7 fb^{-1} of candidate $t\bar{t}$ events in the dilepton and lepton plus jets channels collected by the D0 detector at the Fermilab Tevatron $p\bar{p}$ Collider. We reconstruct the angle θ^* between the momenta of the down-type fermion and the top quark in the W boson rest frame for each top quark decay. A fit of the resulting $\cos\theta^*$ distribution finds that the fraction of longitudinal W bosons $f_0 = 0.490 \pm 0.106$ (stat.) ± 0.085 (syst.) and the fraction of right-handed W bosons $f_+ = 0.110 \pm 0.059$ (stat.) ± 0.052 (syst.), which is consistent at the 23% C.L. with the standard model.

Preliminary Results for Summer 2008 Conferences

The top quark (see footnote [1]) is by far the heaviest of the known fermions and is the only one that has a Yukawa coupling to the Higgs boson of order unity in the standard model (SM). In the SM, the top quark decays via the $V-A$ charged-current interaction, almost always to a W boson and a b quark. We search for evidence of new physics in the $t \to Wb$ decay by measuring the helicity of the W boson. A different Lorentz structure of the $t \to Wb$ interaction would alter the fractions of W bosons produced in each polarization state from the SM values of 0.697 ± 0.012 [2] and 3.6×10^{-4} [3] for the longitudinal fraction f_0 and positive fraction f_+, respectively, at the world average top quark mass m_t of 172.6 ± 1.4 GeV [4].

We report a simultaneous measurement of f_0 and f_+ (the negative helicity fraction f_- is then fixed by the requirement that $f_- + f_0 + f_+ = 1$). A measurement of the W boson helicity fractions that differs significantly from the SM values would be an unambiguous indication of new physics. Examples of models that predict deviations from the SM helicity fractions are presented in Refs. [5], [6], and [7]. In addition, the model-independent W boson helicity measurement can be combined with measurements of single top production cross sections to fully specify the tbW vertex [8].

Measurements of the $b \to s\gamma$ decay rate assuming the absence of gluonic penguin contributions have indirectly limited the $V+A$ contribution in top quark decays to less than a few percent [9]. Previous measurements of the W boson helicity have found $f_0 = 0.65 \pm 0.19$, $f_+ = -0.03 \pm 0.08$ [10] and $f_0 = 0.43 \pm 0.20$, $f_+ = 0.12 \pm 0.10$ [1]. The analysis presented here uses essentially the same procedure reported in Ref. [1], with a data sample that has more than doubled since that publication.

The angular distribution of the down-type decay products of the W boson (charged lepton or d, s quark) in the rest frame of the W boson can be described by introducing the decay angle θ^* of the down-type fermion with respect to the top quark direction. The dependence of the distribution of $\cos\theta^*$ on the W boson helicity fractions,

$$\omega(c) \propto 2(1-c^2)f_0 + (1-c)^2 f_- \ + (1+c)^2 f_+, \tag{1}$$

where $c = \cos\theta^*$, forms the basis for our measurement. We proceed by selecting a data sample enriched in $t\bar{t}$ events, reconstructing the four vectors of the two top quarks and their decay products, and then calculating $\cos\theta^*$. The down-type fermions in leptonic W boson decays are the charged leptons. For hadronic W boson decays, we do not know which of the jets from the W boson arose from a down-type quark, so we choose a jet at random to calculate $\cos\theta^*$. Since this introduces a sign ambiguity into the calculation, we consider only $|\cos\theta^*|$ for hadronic W boson decays. The $|\cos\theta^*|$ variable does not discriminate between left- and right-handed W bosons, but adds information for determining the fraction of longitudinal W bosons. These distributions in $\cos\theta^*$ are compared with templates for different W boson helicity models, suitably corrected for background and reconstruction effects, using a binned maximum likelihood method.

This measurement uses a data sample recorded with the D0 experiment that corresponds to an integrated luminosity of $2.2 - 2.7$ fb^{-1} of $p\bar{p}$ collisions at $\sqrt{s} = 1.96$ TeV. The D0 detector is described elsewhere [11], and underwent significant enhancement in 2006 (in particular, an additional layer of silicon microstrip detectors was installed very close to the beam pipe, and the trigger system was substantially upgraded). Due to these changes, we split the data into "Run IIa" and "Run IIb" subsamples, denoting data recorded before and after the detector enhancement. We have not re-analyzed the ≈ 1 fb^{-1} Run IIa sample for the measurement reported here; rather the result from the Run IIb subset is combined with the Run IIa result from Ref. [1]. Most of the events we use were selected by the trigger system based on the presence of energetic leptons or jets. The Run IIb data sample consists of 1.2 fb^{-1} of $t\bar{t}$ candidate events from the lepton plus jets (ℓ+jets) decay channel $t\bar{t} \to W^+W^-b\bar{b} \to \ell\nu q\bar{q}'b\bar{b}$ and 1.7 fb^{-1} of candidate events in the $e\mu$ channel $t\bar{t} \to W^+W^-b\bar{b} \to e\nu_e\mu\nu_\mu b\bar{b}$ (in the Run IIa analysis, the ee and $\mu\mu$ channels were also used). The ℓ+jets final state is characterized by one charged lepton, at least four jets, and large missing transverse energy ($\not\!\!E_T$). The $e\mu$ final state is characterized by two charged leptons of opposite sign, at least two jets, and large $\not\!\!E_T$. In both final states, at least two of the jets are b jets. Electrons are required to have pseudorapidity [12] $|\eta| < 1.1$ in the ℓ+jets channel and $|\eta| < 1.1$ or $1.5 < |\eta| < 2.5$ in the $e\mu$ channel, and are identified by their energy deposition and isolation in the calorimeter, their transverse and longitudinal shower shapes, and information from the tracking system. Also, a discriminant combining the above information must be consistent with the expectation for a high-p_T isolated electron [13]. Muons are identified using information from the muon and tracking systems and must satisfy isolation requirements based on the energies of calorimeter clusters and the momenta of tracks around the muon. They are required to have $|\eta| < 2.0$ and to be isolated from jets. Jets are reconstructed using a cone algorithm with cone radius 0.5 [14] and are required to have rapidity $|y| < 2.5$ and $p_T > 20$ GeV. The $\not\!\!E_T$ is calculated from the vector sum of calorimeter cell energies, corrected to account for the response of the calorimeter to jets and electrons and also for the momenta of identified muons.

The ℓ+jets event selection [13] requires an isolated lepton (e or μ) with transverse momentum $p_T > 20$ GeV, no other lepton with $p_T > 15$ GeV in the event, $\not\!\!E_T > 20$ GeV, and at least four jets. In the $e\mu$ channel, events are required to have two leptons with opposite charge and $p_T > 15$ GeV and two or more jets.

TABLE I: Summary of the multivariate selection and number of selected events for each of the $t\bar{t}$ final states in the Run IIb data used in this analysis. The uncertainties are statistical only.

	e+jets	μ+jets	$e\mu$
Variables used in discriminant $\mathcal{D}$	$\mathcal{A}$, H_T, h $\langle NN_b\rangle$, $m_{jj\mathrm{min}}$	$\mathcal{A}$, $\mathcal{S}$, h, $m_{jj\mathrm{min}}$, $\langle p_{\mathrm{PV}}\rangle$, $\langle NN_b\rangle$	$\mathcal{C}$, $\mathcal{S}$, h, $m_{jj\mathrm{min}}$, $k'_{T\mathrm{min}}$, NN_{b_1}, $m_{\ell\ell}$
Signal purity before $\mathcal{D}$ selection	0.31 ± 0.05	0.37 ± 0.05	0.66 ± 0.07
Requirement on $\mathcal{D}$	> 0.50	> 0.20	> 0.08
Background after $\mathcal{D}$ selection	88.7 ± 4.5	80.6 ± 5.2	11.4 ± 2.0
Data events after $\mathcal{D}$ selection	251	247	45

We simulate $t\bar{t}$ signal events with $m_t = 172.5$ GeV for different values of f_+ with the ALPGEN Monte Carlo (MC) program [15] for the parton-level process (leading order) and PYTHIA [16] for gluon radiation and subsequent hadronization. We generate samples corresponding to each of the three W boson helicity states by reweighting the generated $\cos\theta^*$ distributions. Backgrounds in the ℓ+jets channel arise predominantly from W+jets production and multijet production where one of the jets is misidentified as a lepton and spurious $\not\!\!E_T$ appears due to mismeasurement of the transverse energy in the event. In the $e\mu$ channel, backgrounds arise from processes such as WW+jets or $Z \to \tau\tau$+jets. The MC samples used to model background events with real leptons are also generated using ALPGEN and PYTHIA. Both the signal and background MC samples are passed through a detailed GEANT3 [17] simulation of the detector response and reconstructed with the same algorithms used for data. To reflect the changes in the detector and reconstruction algorithms between Run IIa and Run IIb, we generate separate samples to model the two data subsamples. In the ℓ+jets channel we estimate the number N_{mj} of multijet background events directly from data, using the technique described in Ref. [13]. We calculate N_{mj} for each bin in the $\cos\theta^*$ distribution from the data sample to obtain the multijet $\cos\theta^*$ templates.

To increase the signal purity following the above selection, a multivariate likelihood discriminant $\mathcal{D}$ [13, 20] with values in the range 0 to 1 is calculated using input variables which exploit differences between signal and background in kinematics and jet flavor. The kinematic variables considered are: H_T (defined as the scalar sum of the jet p_T values), centrality $\mathcal{C}$ (the ratio of H_T to the sum of the jet energies), $k'_{T\mathrm{min}}$ (the distance in $\eta - \phi$ space between the closest pair of jets multiplied by the E_T of the lowest-E_T jet in the pair and divided by the E_T of the W boson), the sum of all jet and charged lepton energies h, the minimum dijet mass of the jet pairs $m_{jj\mathrm{min}}$, aplanarity $\mathcal{A}$, sphericity $\mathcal{S}$ [18], $\not\!\!E_T$, and the $e\mu$ invariant mass $m_{e\mu}$.

We utilize the fact that jets in background events arise mostly from light quarks or gluons while two of the jets in $t\bar{t}$ events arise from b quarks both by calculating the probabilty p_{PV} for the set of tracks within a jet to originate from the primary vertex, and by forming a neural network discriminant between b and light jets [19]. Inputs to this neural network include track impact parameters and the properties of any secondary decay vertices reconstructed within the jet cone. The output is a value NN_b that tends towards one for b jets and towards zero for light jets. In the ℓ+jets channels we use the averages of the two largest NN_b and two smallest p_{PV} values to form continuous variables $\langle NN_b\rangle$ and $\langle p_{\mathrm{PV}}\rangle$. $\langle NN_b\rangle$ tends to be large for $t\bar{t}$ events and small for backgrounds, and the reverse is true for $\langle p_{\mathrm{PV}}\rangle$. In the $e\mu$ channel the NN_b values for the two leading jets (NN_{b_1}, NN_{b_2}) are taken as separate variables. Including these continuous variables in the discriminant results in similar background discrimination but better efficiency than applying a simple cut on either NN_b or p_{PV}.

The discriminant is built separately for each of the three final states considered, using the method described in Refs. [13, 20]. Background events tend to have $\mathcal{D}$ values near 0, while $t\bar{t}$ events tend to have values near 1. We consider all possible combinations of the above variables for use in the discriminant, and all possible requirements on the $\mathcal{D}$ value, and choose the variables and $\mathcal{D}$ criterion that give the best expected precision for the W boson helicity. The variables chosen and the requirement placed on $\mathcal{D}$ for each channel are given in Table I. An example of the distributions of signal, background and Run IIb data events in $\mathcal{D}$ is shown in Fig. 1.

We then perform a binned Poisson maximum likelihood fit to compare the observed distribution of events in $\mathcal{D}$ to the sum of the distributions expected from $t\bar{t}$ and background events. In the ℓ+jets channels, N_{mj} is constrained to the expected value within the known uncertainty, while in the $e\mu$ channel the ratio of the various background sources is fixed to the expectation from the cross sections times efficiency of the kinematic selection. The likelihood is then maximized with respect to the numbers of $t\bar{t}$ and background events, which are multiplied by the efficiency for the $\mathcal{D}$ selection to determine the composition of the sample used for measuring the W boson helicity fractions. Table I lists the composition of each sample as well as the number of observed events in the data.

The top quark and W boson four-momenta in the selected ℓ+jets events are reconstructed using a kinematic fit which is subject to the following constraints: two jets must form the invariant mass of the W boson [21], the invariant mass of the lepton and neutrino must be the W boson mass, and the masses of the two reconstructed top quarks

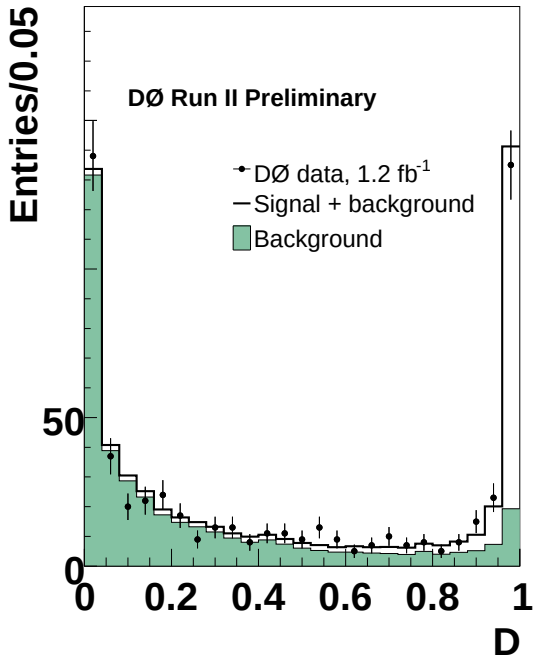

FIG. 1: Distribution of $\mathcal{D}$ for Run IIb data (points with error bars), background (shaded histogram), and signal plus background (open histogram) in the e+jets channel.

must be 172.5 GeV. The four highest-p_T jets in each event are used in the fit, and among the twelve possible jet combinations, the solution with the maximal probability, considering both the χ^2 from the kinematic fit and the NN_b values of the four jets, is chosen. The $\cos\theta^*$ distributions for leptonic and hadronic W boson decays obtained in the ℓ+jets data after the full selection are shown in Fig. 2(a) and (b).

Since the two neutrinos in the $e\mu$ final state are not detected, the system is kinematically underconstrained. However, if a top quark mass is assumed, the kinematics can be solved algebraically with a four-fold ambiguity in addition to the two-fold ambiguity in pairing jets with leptons. For each of the two leading jets, we calculate the value of $\cos\theta^*$ resulting from each solution with each of the two leptons associated with the jet. To explore the phase space consistent with the measured jet and lepton energies, we fluctuate them according to their resolution many times, and repeat the above procedure for each fluctuation. The average of these values is taken as $\cos\theta^*$ for that jet. The $\cos\theta^*$ distribution obtained in $e\mu$ data is shown in Fig. 2(c).

To extract f_0 and f_+, we compute the binned Poisson likelihood $L(f_0, f_+)$ for the data to be consistent with the sum of signal and background templates at any given value for these fractions. The background normalization is constrained to be consistent within uncertainties with the expected value by a Gaussian term in the likelihood. The fit also accounts for the differences in selection efficiency for $t\bar{t}$ events with different W helicity configurations.

Systematic uncertainties are evaluated in ensemble tests by varying the parameters that can affect the shapes of the $\cos\theta^*$ distributions or the relative contribution from signal and background sources. Ensembles are formed by drawing events from a model with the parameter under study varied. These are compared to the standard $\cos\theta^*$ templates in a maximum likelihood fit. The average shifts in the resulting f_0 and f_+ values are taken as the systematic uncertainty and are shown in Table II. The total systematic uncertainty is then taken into account in the likelihood by convoluting the latter with a Gaussian with a width that corresponds to the total systematic uncertainty. The mass of the top quark is varied by ± 1.4 GeV, and the jet reconstruction efficiency, energy calibration, and b fragmentation parameters by $\pm 1\sigma$ around their nominal values. The effect of gluon radiation in the modeling of $t\bar{t}$ events is studied by comparing $t\bar{t}$ events generated by PYTHIA to the standard ALPGEN samples. We also consider samples with a different model for the underlying event and ones in which only a single primary vertex is reconstructed (to estimate the sensitivity of the measurement to variations in instantaneous luminosity). All of these effects are included in the "$t\bar{t}$ model" uncertainty in Table II. Effects of mis-modeling the background distribution in $\cos\theta^*$ are assessed by comparing data to the background model for events with low $\mathcal{D}$ values. The uncertainty due to template statistics is evaluated by fluctuating the templates according to their statistical uncertainties and repeating the fit to the data for each fluctuation. Uncertainties due to jet resolution, jet flavor composition in the background, the modeling of the

TABLE II: Summary of the major systematic uncertainties on f_0 and f_+ in the model-independent fit for the full data sample (Run IIa plus Run IIb).

Source	Uncertainty (f_0)	Uncertainty (f_+)
Top mass	0.009	0.016
Jet reconstruction eff.	0.018	0.009
Jet energy calibration	0.029	0.019
Jet energy resolution	0.023	0.008
$t\bar{t}$ model	0.055	0.028
Background model	0.039	0.026
Template statistics	0.028	0.014
Total	0.085	0.052

NN_b variable, and parton distribution functions are all found to be less than 0.01 for both f_0 and f_+.

The measured values of f_0 and f_+ in the Run IIb sample are:

$$\begin{aligned} f_0 &= 0.538 \pm 0.139\ (\text{stat.}) \pm 0.080\ (\text{syst.}) \\ f_+ &= 0.104 \pm 0.076\ (\text{stat.}) \pm 0.066\ (\text{syst.}), \end{aligned}$$

and the combined Run IIa and Run IIb result is:

$$\begin{aligned} f_0 &= 0.490 \pm 0.106\ (\text{stat.}) \pm 0.085\ (\text{syst.}) \\ f_+ &= 0.110 \pm 0.059\ (\text{stat.}) \pm 0.052\ (\text{syst.}). \end{aligned}$$

The correlation coefficient of f_0 and f_+ is -0.8. The 68%, and 95% C.L. contours from the fit, including systematic uncertainties, are shown in Fig. 3. The data indicate fewer longitudinal and more right-handed W bosons than the SM predicts, but the difference is not statistically significant as there is a 23% chance of observing a larger discrepancy given the statistical and systematic uncertainties in the measurement.

We have also studied splitting the data into various subsamples. We find good consistency between the Run IIa and Run IIb subsets (p-value of 49%), but marginal consistency between the e+jets and μ+jets samples (12%) and between the dilepton and lepton plus jets subsamples (1.6%).

In summary, we have measured the helicity fractions of W bosons in $t\bar{t}$ decays in the ℓ+jets and dilepton channels with a model-independent fit and find $f_0 = 0.490 \pm 0.106$ (stat.) $\pm$ 0.085 (syst.) and $f_+ = 0.110 \pm 0.059$ (stat.) $\pm$ 0.052 (syst.). This is the most accurate such measurement reported and is consistent at the 23% level with the SM values of $f_0 = 0.697$ and $f_+ = 3.6 \times 10^{-4}$.

We thank the staffs at Fermilab and collaborating institutions, and acknowledge support from the DOE and NSF (USA); CEA and CNRS/IN2P3 (France); FASI, Rosatom and RFBR (Russia); CAPES, CNPq, FAPERJ, FAPESP and FUNDUNESP (Brazil); DAE and DST (India); Colciencias (Colombia); CONACyT (Mexico); KRF and KOSEF (Korea); CONICET and UBACyT (Argentina); FOM (The Netherlands); Science and Technology Facilities Council (United Kingdom); MSMT and GACR (Czech Republic); CRC Program, CFI, NSERC and WestGrid Project (Canada); BMBF and DFG (Germany); SFI (Ireland); The Swedish Research Council (Sweden); CAS and CNSF (China); Alexander von Humboldt Foundation; and the Marie Curie Program.

[a] Visitor from Augustana College, Sioux Falls, SD, USA.
[b] Visitor from The University of Liverpool, Liverpool, UK.
[c] Visitor from ICN-UNAM, Mexico City, Mexico.
[d] Visitor from II. Physikalisches Institut, Georg-August-University Göttingen, Germany.
[e] Visitor from Helsinki Institute of Physics, Helsinki, Finland.
[f] Visitor from Universität Zürich, Zürich, Switzerland.
[†] Fermilab International Fellow.
[‡] Deceased.

[1] D0 Collaboration, V. M. Abazov *et al.*, Phys. Rev. Lett. **100**, 062004 (2008). The introductory material and description of the analysis procedure presented here first appeared in this publication.

[2] G. L. Kane, G. A. Ladinsky, and C.-P. Yuan, Phys. Rev. D **45**, 124 (1992); R. H. Dalitz and G. R. Goldstein, *ibid.*, 1531; C. A. Nelson *et al.*, Phys. Rev. D **56**, 5928 (1997).
[3] M. Fischer *et al.*, Phys. Rev. D **63**, 031501(R) (2001).
[4] TeVatron Electroweak Working Group, arXiv:0803.1683 [hep-ex] (2008).
[5] J. Cao *et al.*, Phys. Rev. D **68**, 054019 (2003).
[6] Y.M. Nie *et al.*, Phys. Rev. D **71**, 074018 (2005).
[7] X. Wang, Q. Zhang, and Q. Qiao, Phys. Rev. D **71**, 014035 (2005).
[8] C.-R. Chen, F. Larios, and C.-P. Yuan, Phys. Lett. B **631**, 126 (2005); D0 Collaboration, V.M. Abazov *et al.* Phys. Rev. Lett. **98**, 181802 (2007).
[9] K. Fujikawa and A. Yamada, Phys. Rev. D **49**, 5890 (1994); P. Cho and M. Misiak, Phys. Rev. D **49**, 5894 (1994); C. Jessop, SLAC-PUB-9610 (2002).
[10] CDF Collaboration, S. Moed *et al.*, CDF conference note 9215 (2008).
[11] D0 Collaboration, V. M. Abazov *et al.*, Nucl. Instrum. Methods A **565**, 463 (2006).
[12] Rapidity y and pseudorapidity η are defined as functions of the polar angle θ with respect to the proton beam and the parameter β as $y(\theta,\beta) \equiv \frac{1}{2}\ln[(1+\beta\cos\theta)/(1-\beta\cos\theta)]$ and $\eta(\theta) \equiv y(\theta,1)$, where β is the ratio of a particle's momentum to its energy.
[13] D0 Collaboration, V. M. Abazov *et al.*, Phys. Lett. B **626**, 45 (2005).
[14] G.C. Blazey *et al.*, arXiv:hep-ex/0005012 (2000).
[15] M. L. Mangano *et al.*, JHEP **07**, 001 (2003).
[16] T. Sjöstrand *et al.*, Comp. Phys. Commun. **135**, 238 (2001).
[17] S. Agostinelli *et al.*, Nucl. Instrum. Methods A **506**, 250 (2003).
[18] V. Barger *et al.*, Phys. Rev. D **48**, 3953 (1993).
[19] T. Scanlon, Ph.D. thesis, University of London; FERMILAB-THESIS-2006-43 (2006).
[20] D0 Collaboration, B. Abbott *et al.*, Phys. Rev. D **58**, 052001 (1998).
[21] Review of Particle Physics, W. M. Yao *et al.*, J. Phys. G **33**, 1 (2006).

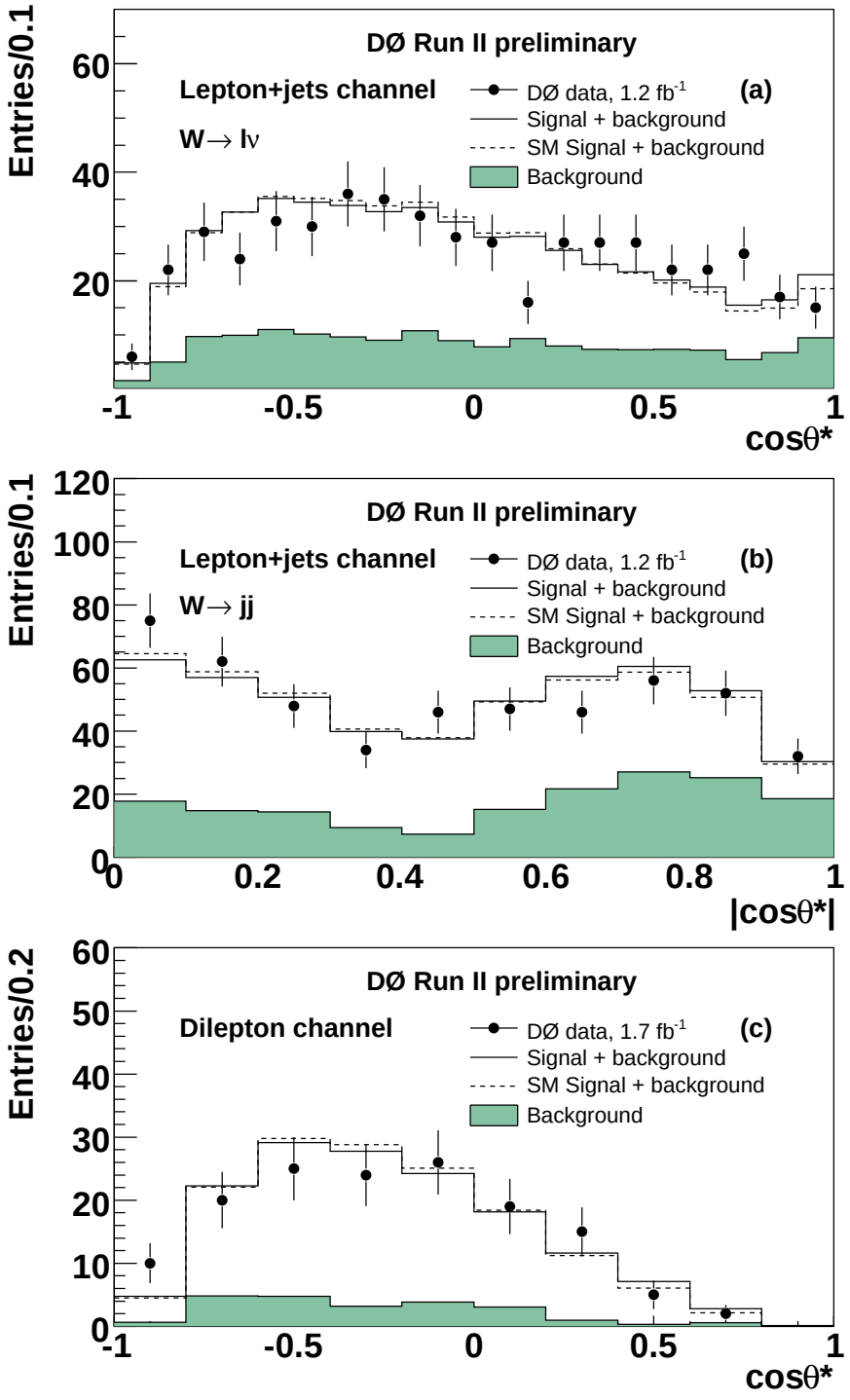

FIG. 2: Comparison of the $\cos\theta^*$ distribution in Run IIb data (points with error bars) and the global best-fit model (solid open histograms) for (a) leptonic W boson decays in ℓ+jets events, (b) hadronic W boson decays in ℓ+jets events, and (c) $e\mu$ events. The dashed open histograms show the SM expectation, and the shaded histograms represent the background contribution.

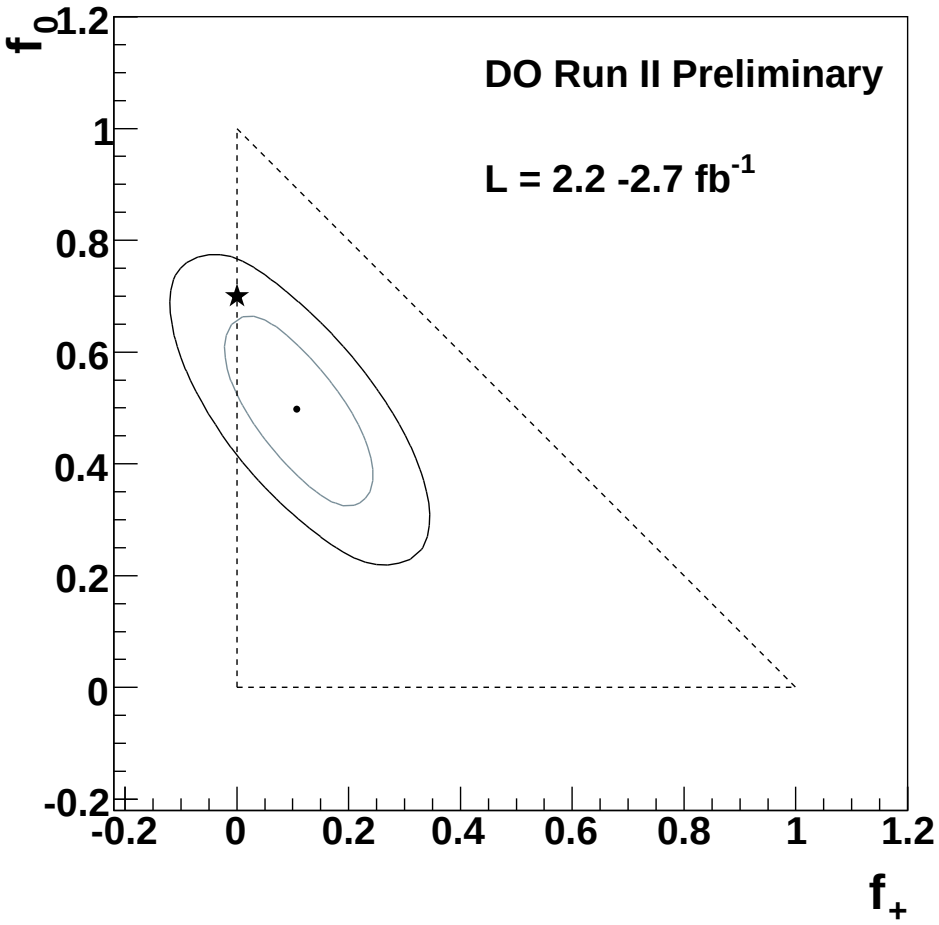

FIG. 3: Result of the model-independent W boson helicity fit for the combined Run IIa and Run IIb samples. The ellipses are the 68% and 95% C.L. contours, the triangle borders the physically allowed region where f_0 and f_+ sum to one or less, and the star denotes the SM values.